Vortices in nonlocal Gross–Pitaevskii equation

2004 J. Phys. A: Math. Gen. 37 6633

(http://iopscience.iop.org/0305-4470/37/26/003)

INSTITUTE OF PHYSICS PUBLISHING JOURNAL OF PHYSICS A: MATHEMATICAL AND GENERAL

J. Phys. A: Math. Gen. **37** (2004) 6633–6651 PII: S0305-4470(04)65620-4

Vortices in nonlocal Gross–Pitaevskii equation

Valery S Shchesnovich[1,2] **and Roberto A Kraenkel**[1]

[1] Instituto de Física Teórica, Universidade Estadual Paulista, Rua Pamplona 145, 01405-900 São Paulo, Brazil
[2] Departamento de Física, Universidade Federal de Alagoas, Maceió AL 57072-970, Brazil

E-mail: valery@ift.unesp.br and kraenkel@ift.unesp.br

Received 29 June 2003, in final form 11 May 2004
Published 16 June 2004
Online at stacks.iop.org/JPhysA/37/6633
doi:10.1088/0305-4470/37/26/003

Abstract

We consider vortices in the nonlocal two-dimensional Gross–Pitaevskii equation with the interaction potential having Lorentz-shaped dependence on the relative momentum. It is shown that in the Fourier series expansion with respect to the polar angle, the unstable modes of the axial n-fold vortex have orbital numbers l satisfying $0 < |l| < 2|n|$, as in the local model. Numerical simulations show that nonlocality slightly decreases the threshold rotation frequency above which the nonvortex state ceases to be the global energy minimum and decreases the frequency of the anomalous mode of the 1-vortex. In the case of higher axial vortices, nonlocality leads to instability against splitting with the creation of antivortices and gives rise to additional anomalous modes with higher orbital numbers. Despite new instability channels with the creation of antivortices, for a stationary solution comprised of vortices and antivortices there always exists another vortex solution, composed solely of vortices, with the same total vorticity but with a lower energy.

PACS numbers: 03.75.Lm, 03.75.Nt

1. Introduction

The Gross–Pitaevskii (GP) equation for the order parameter of mean field theory is derived by replacing the interaction potential by the Fermi zero-range pseudo-potential [1, 2] (see also the review [3]). For the gaseous Bose–Einstein condensates (BECs) usage of the pseudo-potential is justified, since the 'gaseousness parameter', ϱa_s^3, where ϱ is the particle density and a_s is the scattering length, is of order 10^{-3}. In a cold dilute gas only binary collisions at low energy are relevant and these collisions are characterized by a single parameter, the s-wave scattering length, independently of the interaction potential.

The predictions of the mean-field theory agree with the experimental results on BEC in dilute gases when both the quantum fluctuations and the cloud of non-condensed atoms can be neglected. In connection with gaseous BECs, the predictions of the GP equation were first analysed in [4], where insightful estimates were given and important scaling relations were established. The mean-field theory was subsequently employed to account for the dynamical properties of BEC in (i) the description [5] of the ballistic expansion of BEC [6] and (ii) a quantitative theoretical account [7] of the condensate excitation spectra observed in [8]. In both cases the agreement with the experiment was within 5% without any fitting parameters. The existence of the macroscopic phase in BEC, which is one of the premises for introduction of the order parameter, was experimentally verified in the interference picture of two BECs in a double-well potential [9]. Importantly, the quantitative results of this experiment were reproduced within the GP-based mean-field theory [10].

The correspondence between theory and experiment was enhanced dramatically with the observation of quantized vortices. Vortices are experimentally created in BEC using various techniques of orbital momentum transfer to the condensate, such as 'phase imprinting' in a two-component condensate [11], using a laser beam stirrer [12–14], through the decaying solitons into vortex rings [15, 16], rotation of the magnetic trap [17] and rotation of the thermal cloud during the evaporating cooling process [18]. Recently, coreless vortices were produced by the phase imprinting method in a spinor condensate [19].

The mean-field theory which accounts for the mechanism of the angular momentum transfer to the condensate describes the experiments on vortices in gaseous BECs. First the vortex state must have lower energy in the rotating frame than the condensate without vortices. This scenario resulted in the first proposed critical rotation frequency Ω_v [20] for observation of vortices. However, it was shown later that the nonvortex state remains a local minimum at rotation frequencies higher than Ω_v [21] and, hence, an energy barrier may prevent nucleation of vortices. Also, vortex precession around the centre of the trap was identified with its anomalous mode in [22]. A surface mode version of the Landau theory was then suggested as a mechanism for vortex nucleation [23] resulting in a much higher critical nucleation frequency, defined as a minimum over all resonances with surface modes of orbital numbers l and frequencies ω_l: $\Omega_c = \min(\omega_l/l)$. The surface mode theory is generally consistent with the experiments [11–13, 17]. The dynamic vortex formation theory in which a rotating atomic cloud plays an essential role was proposed in [24, 25]. The general vortex–nonvortex state stability diagram for finite temperatures was obtained in [26]. The surface mode spectrum at finite temperatures was computed in [27] within the Popov version of the Hartree–Fock–Bogoliubov theory. It was found that the thermodynamic frequency Ω_v and the critical nucleation frequency Ω_c of the surface-mode theory increase with temperature (however, the nucleation frequency due to the quadrupole mode remains almost unaffected). In [28, 29] extensive numerical simulations of the GP equation and the Bogoliubov linear equations in spherically and cylindrically symmetric traps were performed, where the critical vortex nucleation frequencies were found.

The excitation of surface modes is not the only possible mechanism for vortex nucleation. The action of a localized perturbation, a small stirrer, can allow for vortex formation below the nucleation threshold Ω_c of the surface-mode theory. In the experiment of [14], a nearly pure condensate was excited by a stirrer with variable characteristic size. Rapid nonresonant vortex formation was observed for small stirrer size at a rotation frequency lower than Ω_c, indicating a local mechanism related to the formation of vortex–antivortex pairs (see also [30]). In [31] a classical solid-body model for the angular momentum build-up was shown to describe the above experiment when the density of vortices is high.

In connection with the applicability of the GP equation, an important mathematical result was also established: the Gross–Pitaevskii functional is the asymptotic limit for gaseous BECs of the N-particle energy functional both in three [32] and in two [33] dimensions (see also [34]).

The concept of quantized vortices first appeared in connection with liquid helium in the pioneering ideas of Onsager and Feynman [35] (see also [36–38]). Quantized vortices were experimentally detected in liquid helium [39]. Similar to gases, single vortices and vortex arrays are observed in helium II (for instance, via the ion trapping technique [40, 41]); this subject is reviewed in [36].

Liquid helium, in contrast to cold alkali gases, is a dense strongly correlated system (the parameter ϱa_s^3 is of order 0.1). In helium the interatomic distance is of the order of the interaction range (see, for instance, table I in [42]). The strong dissimilarity between the two systems manifests itself in the vortex core size: the vortex core in gases is much larger than the average interatomic distance, while in liquid helium it is of the same order. Evidently, there is no justification for neglecting the range of interaction in the description of the macroscopic properties of liquid helium.

Several mean field functionals for superfluid helium are discussed in the literature [43–47] (consult also the review [42]). The simplest form of the correlation energy part for liquid helium is as follows [43],

$$\mathcal{E}_c[\varrho] = \int \mathrm{d}^3\mathbf{r} \left\{ \frac{b}{2}\varrho^2 + \frac{c}{2}\varrho^{2+\gamma} + d(\nabla\varrho)^2 \right\} \tag{1}$$

where ϱ is the local density, and b, c and γ are phenomenological parameters. Note that the last term in (1) accounts for the nonlocal interactions in liquid helium and is crucial for the correct description of its macroscopic properties [44, 46]. Instead of the gradient nonlocality as in (1), an *ad hoc* potential with fitting parameters was also proposed [47]. The higher order term $\varrho^{2+\gamma}$ is essential for counteraction of the non-physical mass concentrations in a nonlocal model with attractive–repulsive interactions [48]. Thus, complicated density functionals are proposed to explain the properties of liquid helium. However, it has been known for quite some time that some aspects of vortex dynamics in liquid helium, such as the annihilation of vortex rings [49], the nucleation of vortices [50], the vortex line reconnection [51] and the superfluid turbulence [52], are in fact captured by the local GP model.

In this paper we study the effect of the finite-range of interaction on vortices. Our motivation is that, on one hand, some properties of vortices in the strongly interacting systems seem to be described by the local model and, on the other hand, since vortices appear due to balance between the dispersion and nonlinearity, modification of the interaction potential may lead to different stability properties of vortices. Thus our goal is to find out what changes in the stability properties of vortices can be attributed solely to nonlocality.

Vortices in a nonlocal model were studied recently in [47, 53], where a phenomenological potential was used which brought into agreement the vortex core size with the healing length and allowed us to reproduce the Landau phonon–roton dispersion curve. Our nonlocal model is obtained by substitution of the Fermi zero-range potential by the Yukawa finite-range repulsive potential (the Macdonald function in two dimensions). As we study only the effect of the interaction range, we adopt the simplest model of a nonlocal interaction potential without the attractive part. Thus, we can drop the higher order nonlinear term used to compensate collapse due to attraction. To facilitate the comparison with the local theory we will keep the external confining potential in our nonlocal GP equation (the effects solely due to nonlocality are independent of the external potential). For reasons of accuracy of the numerical analysis, we restrict ourselves to the two-dimensional model (which corresponds to oblate geometry of the system).

The nonlocal GP theory was also recently used to study the effect of nonlocality of the attractive atomic interactions on stability of the ground state against collapse. It is found that nonlocality suppresses collapse [54] and is responsible for the appearance of stable self-trapped configurations [55, 56].

The paper is organized as follows. In section 2 we argue that the simplest finite-range interaction potential is the Yukawa potential (in 3D) and find the corresponding potential in 2D. Then, in section 3, we show that the unstable orbital modes of the axial n-fold vortex have orbital numbers l satisfying $0 < |l| < 2|n|$, while the ground state is spectrally stable—precisely as in the local theory. In section 4 we first numerically study the effect of the interaction range on the critical thermodynamic frequency Ω_v and the stabilization frequency of the 1-vortex. Then we consider the effect of nonlocality on the stability properties of axial 2- and 3-vortices and look for vortex–antivortex solutions corresponding to the n-vortex splitting instabilities caused by the nonlocality for various values of the vorticity n. Section 5 contains concluding remarks.

2. Nonlocal Gross–Pitaevskii model

The Fermi pseudo-potential (given by the Dirac distribution) has one parameter—the scattering length. Thus, the simplest model which can describe nonlocal repulsive interactions involves introduction of an effective potential with two parameters: the strength of interaction and the interaction range. The symmetry property and assumption of short-range interaction allow us to single out the effective potential with two parameters. Indeed, the contribution to the energy functional due to the atomic interactions reads

$$\mathcal{E}_{\rm int} = \frac{g}{2}\int \mathrm{d}^3\mathbf{r}\int \mathrm{d}^3\mathbf{r}'|\Psi(\mathbf{r})|^2 K(\mathbf{r}',\mathbf{r})|\Psi(\mathbf{r}')|^2. \tag{2}$$

Here g is the strength of interactions and the kernel is normalized as $\int \mathrm{d}^3\mathbf{r}K(\mathbf{r}) = 1$. For the spherically symmetric interaction the kernel K depends only on the relative distance: $K = K(|\mathbf{r}' - \mathbf{r}|)$. Its Fourier image is then a real function of the squared wave number $\mathbf{k}$: $\hat{K} = \hat{K}(\mathbf{k}^2)$. In the zero-range limit (the Fermi pseudo-potential) $\hat{K} = 1$. In the next order of the approximation we have $\hat{K} = 1-\epsilon^2\mathbf{k}^2$, where ϵ is the effective interaction range. However, in this form, the expansion has a problem when substituted into the Fourier integral over all $\mathbf{k}$, since the second term is unbounded (the correction would be the dominant term). A remedy for this is to adopt an equivalent expression (up to the next order in ϵ)—the Lorentzian:

$$\hat{K} = (1+\epsilon^2\mathbf{k}^2)^{-1}. \tag{3}$$

The Lorentzian has been used recently as an approximation of the finite-range potential in [55, 56].

Though we will use the Lorentzian in our numerical simulations, the analytical approach presented in this paper is valid for a certain class of interaction potentials to be specified in the next section. The Gaussian

$$\hat{K} = C_\epsilon \exp(-\epsilon^2\mathbf{k}^2) \tag{4}$$

which is another common choice for the phenomenological interaction potential, belongs to our class. In the limit of short-range interactions all the potentials of our class can be approximated by the Lorentzian (3).

In three dimensions the Lorentzian corresponds to the Yukawa effective potential ($a \equiv \epsilon$)

$$K_{\rm 3D} = \frac{1}{4\pi a^2 r}\exp\left(-\frac{r}{a}\right) \tag{5}$$

while in two dimensions the effective interaction potential is given by

$$K_{2D} = \frac{1}{2\pi a^2} K_0\left(\frac{r}{a}\right) \tag{6}$$

where $K_0(z)$ is the Macdonald function (see, for instance, [57]). The kernels (5) and (6) reduce to the Dirac distribution in the limit of the zero-range interaction:

$$\lim_{a\to 0} K_{3D}(\mathbf{r}) = \delta_{3D}(\mathbf{r}) \qquad \lim_{a\to 0} K_{2D}(\mathbf{r}) = \delta_{2D}(\mathbf{r}). \tag{7}$$

Both kernels (5) and (6) have *integrable* singularity at $r = 0$. This is evident in the case of the Yukawa kernel, whereas for the 2D kernel the following asymptotics hold $K_0(x) \sim \ln(2/x)$ as $x \to 0$ [57]. Hence, due to $\ln(x) = o(x^{-\alpha})$ for all $\alpha > 0$ as $x \to 0$, the integrability property follows.

In the following we will also use the operator form, given as Λ^{-1}, for the effective potentials (5) and (6), which then become the Green functions for the positive-definite operator Λ:

$$\Lambda = 1 - a^2\nabla^2. \tag{8}$$

The corresponding nonlocal GP equation (in the reference frame rotating with frequency Ω) reads

$$\mathrm{i}\hbar\partial_t\Psi = -\frac{\hbar^2}{2m}\nabla^2\Psi + V\Psi - \Omega L_z\Psi + g\Psi\Lambda^{-1}|\Psi|^2. \tag{9}$$

Here L_z is the angular momentum projection on the z-axis: $L_z = -\mathrm{i}\hbar(x\partial_y - y\partial_x) = -\mathrm{i}\hbar\partial_\theta$, where θ is the polar angle in the transverse dimensions. To facilitate comparison with the local model we will use the parabolic external potential confining in the transverse dimensions:

$$V = \frac{m\omega_\perp^2}{2}\rho^2 = \frac{V_0}{a_\perp^2}\rho^2$$

where $\boldsymbol{\rho} \equiv (x, y)$ and $\rho = |\boldsymbol{\rho}|$, $V_0 = \hbar\omega_\perp/2$ is the characteristic energy of the trap and the characteristic length scale is $a_\perp = \sqrt{\hbar/(m\omega_\perp)}$. For simplicity, we consider the periodic boundary conditions along the z-axis, $\Psi(z + d) = \Psi(z)$.

In the following it will be convenient to use the dimensionless variables:

$$t' = \frac{\omega_\perp}{2}t \qquad \mathbf{r}' = \frac{\mathbf{r}}{a_\perp} \qquad \psi = \frac{a_\perp\sqrt{d}}{\sqrt{N}}\Psi \qquad \Omega' = \frac{2\Omega}{\omega_\perp} \qquad L_z' = \frac{L_z}{\hbar} \qquad g' = \frac{gN}{V_0 a_\perp^2 d} \tag{10}$$

Here N is the number of atoms in the condensate per z-period d. Note that the wavefunction ψ is normalized to 1. The interaction range is also normalized by the characteristic length of the transverse potential $a' = a/a_\perp$. Below we will use only the dimensionless form of equation (9), thus we drop the primes in all the variables.

Assuming no dependence on z, the axially symmetric n-fold vortex solution reads $\psi = \mathrm{e}^{\mathrm{i}n\theta - \mathrm{i}\mu t}A(\rho)$ (here A depends on n), with the amplitude A satisfying

$$L_0 A \equiv \left\{-\nabla_\rho^2 + \frac{n^2}{\rho^2} + V(\rho) + gF_0 - (\mu + \Omega n)\right\} A = 0 \tag{11}$$

$$F_0 \equiv \left(1 - a^2\nabla_\rho^2\right)^{-1} A^2 \tag{12}$$

here $\nabla_\rho^2 \equiv \rho^{-1}\partial_\rho\rho\partial_\rho$ is the radial part of the Laplacian in 2D and $2\pi\int_0^\infty \rho\,\mathrm{d}\rho A^2 = 1$.

3. Stability of the axial vortices in nonlocal interactions

The stability properties of the axial n-fold vortices in the local GP equation are well known. In BEC with repulsive interactions the unstable orbital modes $\sim e^{il\theta}$ of the n-vortex in the axisymmetric trap have orbital numbers l satisfying $0 < |l| < 2|n|$ [58] (l is the angular momentum of the mode). The 1-vortex has at least one anomalous mode (exactly one in 2D), i.e. the mode with positive norm and negative energy, qualitatively predicted in [59] and found later in [60]. The number of anomalous modes of the 1-vortex depends on the geometry of the trap: in a prolate trap additional anomalous modes are possible [22, 29], which describe bending of the vortex lines. The detailed phase diagram for vortex stability in 2D was numerically obtained in [21, 26]. The role of the excitations with negative energies in vortex instability was clarified in [61]. Finally, it was numerically found that there are intervals of the interaction strength g where the axial n-vortices with $n \geqslant 2$ are dynamically unstable [62].

These results concern condensates with repulsive interactions. It was also shown that in the *attractive* condensate the 1-vortex solution undergoes splitting due to unstable quadrupole mode [63].

Related issues of vortices in the Ginzburg–Landau equation (which represents nonconservative generalization of the GP equation) were considered in [64–66] and the properties of the optical vortices were reviewed in [67].

Here we show that there is a class of interaction potentials for which the unstable modes of the n-fold axial vortex have orbital numbers in the interval: $0 < |l| < 2|n|$, i.e. exactly as in the local model.

It is convenient to use another form of the nonlocal GP equation with an additional dependent variable F describing the nonlinear term (all equations below are in 2D):

$$(1 - a^2\nabla^2)F = |\psi|^2 \tag{13}$$

$$\{-\mathrm{i}\partial_t - \nabla^2 + V(\rho) - \Omega\tilde{L}_z + gF\}\psi = 0. \tag{14}$$

Here $V = V(\rho)$ is the general confining trap which allows for the axial vortex solutions with the amplitude decreasing to zero as $\rho \to \infty$.

The class of interaction potentials for which the main result below is valid is defined as follows. The general expression for the nonlinear term F, corresponding to the general kernel K, reads

$$F = \int \mathrm{d}^2\boldsymbol{\rho}'\, K(\boldsymbol{\rho}, \boldsymbol{\rho}')|\psi(\boldsymbol{\rho}')|^2. \tag{15}$$

Vortex solutions are possible for the kernels $K = K(|\boldsymbol{\rho}' - \boldsymbol{\rho}|)$. Indeed, the quantity F_0 (a generalization of that in (11)) is given by the following integral:

$$F_0 = \int_0^\infty \rho'\,\mathrm{d}\rho' \left\{ \int_0^{2\pi} \mathrm{d}\theta'\, K([\rho^2 + \rho'^2 - 2\rho\rho'\cos(\theta' - \theta)]^{\frac{1}{2}}) \right\} A^2(\rho'). \tag{16}$$

Obviously, F_0 is a function of ρ only and this fact allows, in principle, existence of the axial vortex solutions.

We consider the class of interaction potentials of the type $K = K(|\boldsymbol{\rho}' - \boldsymbol{\rho}|)$ for which the coefficients of the operator Λ^{-1} in the Fourier expansion with respect to the polar angle are defined as

$$\Lambda_l^{-1} f \equiv \int_0^\infty \rho'\,\mathrm{d}\rho' \left[\int_0^{2\pi} \mathrm{d}\phi \cos(l\phi) K([\rho^2 + \rho'^2 - 2\rho\rho'\cos\phi]^{\frac{1}{2}}) \right] f(\rho')$$
$$l = 0, 1, 2, \ldots, \tag{17}$$

i.e. the radial operators with the kernels given by the expression in the square brackets in (17), are all positive-definite. For example, the Gaussian interaction potential

$$K = \frac{1}{2\pi a^2} \exp\left(-\frac{\rho^2}{2a^2}\right) \tag{18}$$

possesses this property. Indeed, the radial operator Λ_l^{-1} is given by the expression

$$\Lambda_l^{-1} f = \frac{1}{a^2} \int_0^\infty \rho' \, \mathrm{d}\rho' \exp\left(-\frac{\rho'^2 + \rho^2}{2a^2}\right) I_l\left(\frac{\rho\rho'}{2a^2}\right) f(\rho') \tag{19}$$

where $I_l(x)$ is the Bessel function of the second kind. There is a sufficiently large R such that the sign of the quadratic form of the operator Λ_l^{-1} on some $f = f(\rho)$ is given by the sign of the finite integral

$$\int_0^R \int_0^R \mathrm{d}\rho \, \mathrm{d}\rho' \chi(\rho) I_l\left(\frac{\rho\rho'}{2a^2}\right) \chi(\rho')$$

with $\chi \equiv \exp\{-\rho^2/2a^2\}\rho f(\rho)$. Since the Taylor expansion of the modified Bessel function $I_l(\rho\rho'/2a^2)$ is a uniformly convergent series in powers of $\rho\rho'$ with positive coefficients, the positivity of the operator Λ_l (19) follows.

For the interaction potential (6), corresponding to the Lorentzian, the operator Λ_l is given by

$$\Lambda_l = 1 - a^2\left[\nabla_\rho^2 - \frac{l^2}{\rho^2}\right]. \tag{20}$$

Obviously, the radial operators $\Lambda_l, l = 0, 1, 2, \ldots$, are positive definite with respect to the inner product defined by the integral $\int_0^\infty \rho \, \mathrm{d}\rho(\cdot)$.

We assume that the system (11), (16) with a given axisymmetric external potential $V(\rho)$ admits axial n-vortex solutions.

Definition. *We will say that the interaction potential with the kernel $K(|\boldsymbol{\rho}' - \boldsymbol{\rho}|)$ satisfies the positivity property if the associated radial operators Λ_l^{-1} (17), $l = 0, 1, 2, 3, \ldots$, are positive definite.*

Theorem. *The axial n-vortex solution to the system (14), (15) with the interaction potential satisfying the positivity property can be spectrally unstable only with respect to perturbations which have nonzero projection on the orbital basis $\mathrm{e}^{\mathrm{i}l\theta}$ in the interval $0 < |l| < 2|n|$. The ground state solution is spectrally stable.*

Proof. Let us linearize the system (14), (15) about the axial n-vortex solution. Expanding the linear corrections Φ and F_1

$$\psi = \{A(\rho) + \epsilon\Phi(\rho, \theta, t)\}\,\mathrm{e}^{\mathrm{i}n\theta - \mathrm{i}\mu t} \qquad F = F_0(\rho) + \epsilon F_1(\rho, \theta, t) \tag{21}$$

in the Fourier series with respect to θ,

$$\Phi = \sum_{l \geqslant 0} u_l(\rho, t)\,\mathrm{e}^{\mathrm{i}l\theta} + v_l^*(\rho, t)\,\mathrm{e}^{-\mathrm{i}l\theta} \qquad F_1 = \sum_{l \geqslant 0} b_l(\rho, t)\,\mathrm{e}^{\mathrm{i}l\theta} + \text{c.c.} \tag{22}$$

inserting the result into the system (14), (15) and solving for b_l yields the nonlocal Bogoliubov equations for (u_l, v_l):

$$\mathrm{i}\partial_t \begin{pmatrix} u_l \\ v_l \end{pmatrix} = J \begin{pmatrix} L_l + gA\Lambda_l^{-1}A & gA\Lambda_l^{-1}A \\ gA\Lambda_l^{-1}A & L_{-l} + gA\Lambda_l^{-1}A \end{pmatrix} \begin{pmatrix} u_l \\ v_l \end{pmatrix} \equiv J H_l \begin{pmatrix} u_l \\ v_l \end{pmatrix}. \tag{23}$$

Here $J = \mathrm{diag}(1, -1)$, the operators Λ_l^{-1} are understood as acting on the products of Au_l or Av_l, and the operators $L_{\pm l}$ are defined as

$$L_{\pm l} = -\nabla_\rho^2 + V(\rho) + \frac{(n \pm l)^2}{\rho^2} + gF_0 - (\mu + \Omega(n \pm l)). \tag{24}$$

The matrix operator H_l introduced by (23) is real and symmetric and also has the following property:

$$\tau H_l \tau = H_{-l} \qquad \tau \equiv \begin{pmatrix} 0 & 1 \\ 1 & 0 \end{pmatrix}. \tag{25}$$

The operator H_l is related to the orbital projection of the Hessian in the rotating reference frame. Indeed, the solution $\psi = A(\rho)\, \mathrm{e}^{\mathrm{i}n\theta - \mathrm{i}\mu t}$ is the stationary point of the Lagrange-modified energy functional in the rotating frame

$$E \equiv \mathcal{E} - \mu N = \int \mathrm{d}^2\boldsymbol{\rho} \left\{ |\nabla\psi|^2 + V|\psi|^2 - \Omega\psi^* L_z \psi + \frac{g}{2} F|\psi|^2 \right\} - \mu N \tag{26}$$

(i.e. $\delta E/\delta\psi^* = 0$ at the solution) where $N = \int \mathrm{d}^2\boldsymbol{\rho}|\psi|^2$ is the number of atoms. Equation (23) can be obtained from the following one,

$$\mathrm{i}\partial_t \begin{pmatrix} \Phi \\ \Phi^* \end{pmatrix} = J\, \mathrm{e}^{-\mathrm{i}n\theta J} \begin{pmatrix} \frac{\delta^2 E}{\delta\psi\delta\psi^*} & \frac{\delta^2 E}{\delta\psi^*\delta\psi^*} \\ \frac{\delta^2 E}{\delta\psi\delta\psi} & \frac{\delta^2 E}{\delta\psi^*\delta\psi} \end{pmatrix} \mathrm{e}^{\mathrm{i}n\theta J} \begin{pmatrix} \Phi \\ \Phi^* \end{pmatrix} \equiv \mathrm{e}^{-\mathrm{i}n\theta J} H_{ess}\, \mathrm{e}^{\mathrm{i}n\theta J} \begin{pmatrix} \Phi \\ \Phi^* \end{pmatrix} \tag{27}$$

by expansion into the Fourier series with respect to θ. Using this fact and the properties of the operator H_l, one can write the expansion of the Lagrange-modified energy function (26) in powers of ϵ as follows:

$$\begin{aligned} E &= E_0 + \frac{\epsilon^2}{2} \int \mathrm{d}^2\boldsymbol{\rho}(\Phi^*, \Phi)\, \mathrm{e}^{-\mathrm{i}n\theta J} H_{ess}\, \mathrm{e}^{\mathrm{i}n\theta J} \begin{pmatrix} \Phi \\ \Phi^* \end{pmatrix} + \mathcal{O}(\epsilon^3) \\ &= E_0 + 2\pi\epsilon^2 \sum_{l \geqslant 0} \int_0^\infty \rho\, \mathrm{d}\rho(u_l^*, v_l^*) H_l \begin{pmatrix} u_l \\ v_l \end{pmatrix} + \mathcal{O}(\epsilon^3). \end{aligned} \tag{28}$$

For stability according to Lyapunov all the terms in the series in equation (28) must be positive. The n-fold axial vortex solution is spectrally unstable if the radial linear problems

$$J H_l \begin{pmatrix} X_1 \\ X_2 \end{pmatrix} = \mathrm{i}\sigma \begin{pmatrix} X_1 \\ X_2 \end{pmatrix} \qquad l = 0, 1, 2, \ldots \tag{29}$$

allow eigenvalues σ with nonzero real part (the solution associated with the linear system (23) involves the exponent multiplier $\mathrm{e}^{\sigma t}$).

It is helpful to recall the general result on stability of the stationary points of Hamiltonian systems [68]. It is known that (i) the eigenvalues appear in quartets $\Xi \equiv \{\sigma, -\sigma^*, -\sigma, \sigma^*\}$; (ii) the second-order correction to energy taken over the subspace corresponding to a quartet of eigenvalues with a nonzero real part has indefinite signature and (iii) the stationary point may lose the spectral stability only by collision of the (imaginary) eigenvalues bearing signatures of opposite sign or by collision at zero $\sigma = 0$.

With a quartet of eigenvalues $\{\sigma, -\sigma^*, -\sigma, \sigma^*\}$, with σ being the eigenvalue from (29), the following eigenfunctions, additional to those in (29), can be associated:

$$\begin{aligned} &J H_l \begin{pmatrix} X_1^* \\ X_2^* \end{pmatrix} = -\mathrm{i}\sigma^* \begin{pmatrix} X_1^* \\ X_2^* \end{pmatrix} \qquad J H_{-l} \begin{pmatrix} X_2 \\ X_1 \end{pmatrix} = -\mathrm{i}\sigma \begin{pmatrix} X_2 \\ X_1 \end{pmatrix} \\ &J H_{-l} \begin{pmatrix} X_2^* \\ X_1^* \end{pmatrix} = \mathrm{i}\sigma^* \begin{pmatrix} X_2^* \\ X_1^* \end{pmatrix}. \end{aligned} \tag{30}$$

This is due to the fact that H_l is a symmetric real operator possessing property (25). It is easy to establish that all the eigenvalues from a given quartet bear the same signature. The energy corresponding to the eigenfrequency ω ($\sigma = -\mathrm{i}\omega$) is equal to $\omega\langle X|J|X\rangle$ where $\langle X|J|X\rangle = 2\pi\int_0^\infty \rho\,\mathrm{d}\rho(|X_1|^2 - |X_2|^2)$.

For the following it is convenient to get rid of the diagonal terms $-\Omega l$ in the operator JH_l by expanding it as follows (here I is the unit matrix):

$$JH_l = J\widetilde{H}_l - \Omega l I. \tag{31}$$

The new operator $J\widetilde{H}_l$ has the same eigenfunctions, which now correspond to the shifted eigenvalues: $\tilde{\sigma} \equiv \sigma - \mathrm{i}\Omega l$. The stable orbital numbers l correspond to non-negative eigenvalues of $J\widetilde{H}_l J\widetilde{H}_l$ (i.e. $-\tilde{\sigma}^2 \geqslant 0$). (Here we note that the instability with a polynomial growth in time t is not possible in the system (23), since the two eigenvalues σ and $-\sigma$ coinciding at zero belong to different operators, namely JH_l and JH_{-l}, see equation (30).) We will prove the inequality in the theorem by showing that the operator $J\widetilde{H}_l J$ is positive for $|l| \geqslant 2|n|$, $l \neq 0$ and non-negative for $l = 0$ with one zero mode.

Indeed, consider the inner product of $J\widetilde{H}_l J$ with $X = (X_1, X_2)^T$:

$$\begin{aligned}\langle X|J\widetilde{H}_l J|X\rangle = 2\pi\int_0^\infty \rho\,\mathrm{d}\rho\big\{&X_1^*\big(\tilde{L}_l + gA\Lambda_l^{-1}A\big)X_1 + X_2^*\big(\tilde{L}_{-l} + gA\Lambda_l^{-1}A\big)X_2 \\ &- g\big(X_1^* gA\Lambda_l^{-1}AX_2 + X_2^* gA\Lambda_l^{-1}AX_1\big)\big\}\end{aligned} \tag{32}$$

where $\tilde{L}_{\pm l} \equiv L_{\pm l} \pm \Omega l = L_0 + l(l \pm 2n)\rho^{-2}$. The operator L_0 is non-negative. The quickest way to see this is to rewrite L_0 as follows (due to equation (11))

$$L_0 = -\frac{1}{\rho A}\frac{\mathrm{d}}{\mathrm{d}\rho}\rho A^2\frac{\mathrm{d}}{\mathrm{d}\rho}\frac{1}{A} \tag{33}$$

and take into account that, in the inner product defined by the integral $\int\rho\,\mathrm{d}\rho(\cdot)$, the rhs in (33) can be factorized via integration by parts. Using non-negativity of the operator L_0 and dropping the following non-negative term on the rhs of (32)

$$\begin{aligned}&\int_0^\infty \rho\,\mathrm{d}\rho\big\{X_1^* gA\Lambda_l^{-1}AX_1 + X_2^* gA\Lambda_l^{-1}AX_2 - g\big(X_1^* gA\Lambda_l^{-1}AX_2 + X_2^* gA\Lambda_l^{-1}AX_1\big)\big\} \\ &\qquad = \int_0^\infty \rho\,\mathrm{d}\rho\big\{(X_1^* - X_2^*)gA\Lambda_l^{-1}A(X_1 - X_2)\big\} \geqslant 0\end{aligned} \tag{34}$$

(since Λ_l^{-1} is assumed positive in the formulation of the theorem) we arrive at the following inequalities:

$$\begin{aligned}\langle X|J\widetilde{H}_l J|X\rangle &\geqslant 2\pi\int_0^\infty \rho\,\mathrm{d}\rho\left\{\frac{l(l+2n)}{\rho^2}|X_1|^2 + \frac{l(l-2n)}{\rho^2}|X_2|^2\right\} \\ &\geqslant (l^2 - 2|nl|)2\pi\int_0^\infty \frac{\mathrm{d}\rho}{\rho}(|X_1|^2 + |X_2|^2).\end{aligned} \tag{35}$$

(The linear space in which the inner product in inequality (35) exists contains the eigenfunctions. Indeed, (X_1, X_2) represents the radial part of the eigenfunction $(X_1(\rho)\,\mathrm{e}^{\mathrm{i}(l+n)\theta}, X_2(\rho)\,\mathrm{e}^{\mathrm{i}(l-n)\theta})$ (see equations (27) and (22)). Since the latter is regular in the Euclidean variables (x, y), we conclude that for nonzero n and/or l, $X_1 = \mathcal{O}(\rho^{|n+l|})$ and $X_2 = \mathcal{O}(\rho^{|n-l|})$ as $\rho \to 0$, while for the ground state ($n = 0$) $l = 0$, hence the rhs of (35) is zero.)

Let us establish when the inner product $\langle X|J\widetilde{H}_l J|X\rangle$ is zero. Obviously, $\langle X|J\widetilde{H}_0 J|X\rangle = 0$ for $X_1 = X_2 = A$. For general l, the condition $X_1 = X_2 = \kappa A$ (κ is a constant multiplier) is necessary for the dropped terms $X_1^* L_0 X_1 + X_2^* L_0 X_2$ and the rhs of equation (34) to be zero,

i.e. for the first row in formula (35) to be related by the equality sign. But then from the rhs of (35) (the first row) we conclude that $l = 0$, i.e. no additional zero modes are possible. Thus, for $|l| \geqslant 2|n|$ and $l \neq 0$ the operator $J\widetilde{H}_l J$ is strictly positive and for $l = 0$ it is non-negative with one zero mode $X = (A, A)^T$. $\widetilde{H}_l$ is also such as operator, in which case the zero mode is $(A, -A)^T$. Now the eigenvalue problem (29) can be rewritten as follows,

$$\widetilde{H}_l \begin{pmatrix} X_1 \\ X_2 \end{pmatrix} = -\tilde{\sigma}^2 (J\widetilde{H}_l J)^{-1} \begin{pmatrix} X_1 \\ X_2 \end{pmatrix} + \delta_{l,0}\beta \begin{pmatrix} A \\ A \end{pmatrix} \tag{36}$$

where the application of the inverse of $J\widetilde{H}_l J$ to the vector $(X_1, X_2)^T$ on the rhs is justified since for $\tilde{\sigma} \neq 0$ this eigenvector is orthogonal to $(A, A)^T$ by the Fredholm alternative theorem. The minimal eigenvalue of $J\widetilde{H}_l J\widetilde{H}_l$ is therefore defined as

$$\min(-\tilde{\sigma}^2) = \min \frac{\langle X|\widetilde{H}_l|X\rangle}{\langle X|(J\widetilde{H}_l J)^{-1}|X\rangle} \tag{37}$$

where the quotient is minimized in the orthogonal complement to the direction given by $(A, A)^T$. Here we recall that for spectral stability the quotient on the rhs of (37) must take only non-negative values. But the latter quotient is positive for $|l| \geqslant 2|n|$ and $l \neq 0$. For $l = 0$ we have one zero mode $(A, -A)^T$. □

Remark. In the course of the proof we have established positivity of the operators $\widetilde{H}_l$ (the orbital projections of the Hessian for $\Omega = 0$) with $|l| \geqslant 2|n|$ and $l = 0$ for the n-fold axial vortex solution (the zero mode of the operator $\widetilde{H}_0$ corresponds to the invariance of the system (14), (15) with respect to a phase shift).

The established positivity property, however, does not imply the thermal or Lyapunov stability of the ground state for nonzero Ω, since the operators $H_l = \widetilde{H}_l - \Omega l J$ are not, in general, positive.

It is known that there is a threshold value of the rotation frequency above which the ground state loses its Lyapunov stability against the surface mode excitations by a perturbation breaking the rotational symmetry (see [23, 27]). Indeed, this is a consequence of the formula (see equation (31))

$$\langle X|H_l|X\rangle = (\omega - \Omega l)\langle X|J|X\rangle \tag{38}$$

where $\omega \equiv \mathrm{i}\sigma$ is the eigenfrequency of the oscillations with orbital number l in the non-rotating system and X is the corresponding eigenfunction. For fixed l the above instability threshold is given by the quotient $\Omega_l = \omega/l$. For a general perturbation, the critical rotation frequency at which the nonvortex state loses its local stability is thus given by the formula $\Omega_c = \min(\omega_l/l)$, where the minimum is determined over all the resonances with the surface modes [23].

The Hessian corresponding to the nonvortex state possesses an additional property. Setting $n = 0$ in equation (24) we get $L_{\pm l} = L_0 + l^2/\rho^2 \mp \Omega l$ giving

$$H_{-l} = H_l + 2\Omega l J. \tag{39}$$

Therefore, for the nonvortex state at zero rotation ($\Omega = 0$) the partial operators JH_l and JH_{-l} both have complex conjugate pairs of the eigenvalues: $\sigma = \pm\mathrm{i}\omega$.

4. Numerical results

We consider the two-dimensional nonlocal GP model (13) and (14) with the interaction potential corresponding to the Lorentzian. In other words, we restrict ourselves to straight vortex lines, which correspond to oblate geometry—the simplest possible case. Thus, investigation of vortex bending and formation of vortex rings is beyond the scope of the

present paper. Though the results below are given only for the parabolic external potential, we have checked that the addition of a perturbation to the potential does not affect the conclusions on nonlocality-induced effects (see figure 2, for instance). (Similar results on nonlocality-induced instabilities also hold in a completely different external potential—the tangent-shaped trap, which models the weak confinement. For instance, figures 1, 3, 4 and 5 have their counterparts for the tangent trap.)

To study the n-vortex solutions and their spectra within the one-dimensional systems in the radial variable (11), (12) and (23), we have used two pseudo-spectral methods [69] based on the Fourier and Chebyshev expansions and used the Fourier-based method in search for the vortex configurations in 2D. For the radial variable we have used up to 256 grid points (which is the number of Fourier modes and the degree of the Chebyshev polynomial), while the 2D grid was 128×128. The eigenvalues and eigenfunctions of the nonlocal linear problem (23) were found by using the LAPACK routines. To find the n-vortex solutions and the two-dimensional vortex configurations we have minimized the generalized Rayleigh functional (the Rayleigh functional is also known as the Rayleigh quotient in applications to linear systems). For the GP equation the generalized Rayleigh functional is defined as energy functional $\mathcal{E}(\psi)$ evaluated at the normalized function:

$$R(\psi) \equiv \mathcal{E}\left(\frac{\psi}{\|\psi\|}\right) = \int \mathrm{d}^2\boldsymbol{\rho}\left\{|\nabla f|^2 + V|f|^2 - \Omega f^* L_z f + \frac{g}{2}F(f)|f|^2\right\}\Big|_{f=\frac{\psi}{\|\psi\|}} \tag{40}$$

(recall that our interaction coefficient g is in fact gN with N being a fixed number of atoms, see equation (10)). Here the functional $F(\psi)$ is given by equation (15) and $\|\psi\|^2 = \int \mathrm{d}^2\boldsymbol{\rho}|\psi|^2$. By using the Rayleigh functional we achieve two goals: convert the constrained energy minimization problem to an unconstrained minimization problem and fix the number of atoms in the numerical solution. The stationary solutions are extremal points of the Rayleigh functional. Indeed, the variation of the functional $R(\psi)$ reads

$$\frac{\delta R}{\delta \psi^*} = \frac{1}{\|\psi\|}\left[\frac{\delta \mathcal{E}}{\delta f^*} - \mathrm{Re}\left\{\int \mathrm{d}^2\boldsymbol{\rho} f^* \frac{\delta \mathcal{E}}{\delta f^*}\right\} f\right]\Big|_{f=\frac{\psi}{\|\psi\|}}. \tag{41}$$

For a stationary point (extremal point of $R(\psi)$) the integral on the rhs of equation (41) is in fact the corresponding value of the chemical potential (this follows from the stationary GP equation $\mu\psi = \delta\mathcal{E}/\delta\psi^*$, if one takes into account that the interaction coefficient was normalized as $g \to gN$ and that $\psi = \|\psi\| f$). Moreover, it is easy to see that the Rayleigh quotient is also the Lyapunov functional for the local minima (for a fixed number of atoms), since the second variation of $R(\psi)$ is given by the second variation of the 'free energy' functional, defined as $\mathcal{E}(f) - \mu\int \mathrm{d}^2\boldsymbol{\rho} f^2$, with the substitution $\delta f = \delta(\psi/\|\psi\|)$. (The method based on the generalized Rayleigh quotient will be given in more detail in a separate publication [70].) We looked for the absolute energy minimizer by starting from the topologically different initial functions ψ in the minimization procedure and comparing the energy of the resulting local minima. Finally, we checked the accuracy by varying the grid size and observing the changes in the solution, in all cases the error of the numerical solution had a negligible effect on the results.

Let us start with the nonvortex state. One of the characteristic parameters of the nonvortex state is the rotation frequency Ω_v above which it ceases to be the global minimum of the energy functional (in the rotating reference frame). The threshold rotation frequency was numerically computed by comparing the energies of the nonvortex state and the 1-vortex in the rotating frame. The result is presented in figure 1(a) (in our dimensionless system the rotation frequency is measured in halves of the trap frequency, see equation (10)). It is seen

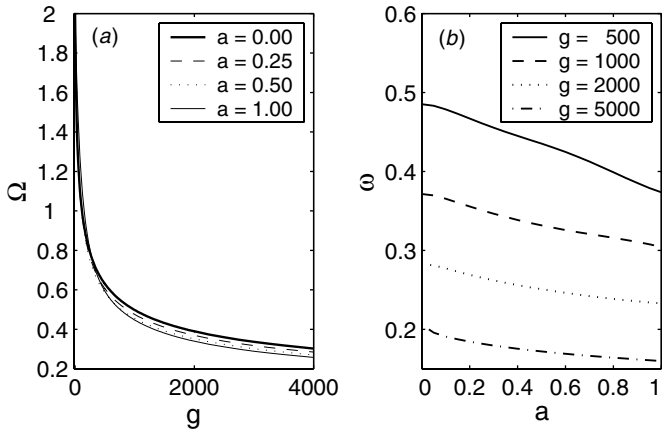

Figure 1. The threshold rotation frequency above which the 1-vortex has lower energy (in the rotating frame) than the nonvortex state versus the strength of interaction for various values of the interaction range (*a*), and the frequency of the anomalous mode (for $\Omega = 0$) of the 1-vortex versus the interaction range for various values of the interaction strength (*b*).

that even an unjustifiably large range of interactions only slightly affects the threshold rotation frequency Ω_v.

We found that the 1-vortex solution has only imaginary eigenvalues $\sigma = -\mathrm{i}\omega$ for all $a \leqslant 1$, thus it is dynamically stable in the nonlocal GP model (13) and (14). It turns out that, similar to the local model, it has one anomalous mode (for $\Omega = 0$), i.e. the eigenvalue corresponding to the orbital operator H_l, with $l = 1$, in equation (23) and with negative energy. The frequency of the anomalous mode decreases with increasing interaction range a, see figure 1(*b*) (here and below, we choose to show the modes of the operators H_l with $l > 0$, thus our 'anomalous mode' has negative norm and positive frequency and is related by equation (30) to the true anomalous mode of the operator H_{-l}). It is known that the frequency of the anomalous mode gives the frequency of vortex precession around the axis of the trap [22]. As was mentioned above, the results on the nonlocality-induced effects do not depend on the external trap. To illustrate this we give the analogue of figure 1(*b*) for the perturbed parabolic trap in figure 2. The 1-vortex solution suffers from a slight deformation with respect to variation of the interaction range as is seen in figure 3.

We now turn to the higher axial n-fold vortices. For the local GP equation it is known that the intervals of the interaction strength g where the axial n-vortex is dynamically unstable are intertwined with the intervals of dynamical stability [62]. According to the main result of section 3, the axial n-vortex solution may be unstable only with respect to the orbital perturbations $\sim \mathrm{e}^{\mathrm{i}l\theta}$ satisfying $0 < l < 2n$ (without loss of generality we can consider only positive n and l). The instabilities of the n-vortices result in vortex splitting. This fact can be seen from the Taylor expansion with respect to $z = x + \mathrm{i}y$ and z^* of the perturbed vortex solution with a perturbation having nonzero projection on the orbital number l (see formulae (21)–(22))—for $0 < l < 2n$ the lowest power in z and/or z^*, which defines the vorticity at the origin, will be $|n - l|$, i.e. will come from the perturbation.

Variation of the interaction range a for any fixed interaction strength g (in physical terms, the interaction strength multiplied by the number of atoms) results in the appearance of a finite number of instability intervals, now with respect to the interaction range, due to resonances of the anomalous and normal modes. We have not found resonances with the orbital number $l = 1$ (which are not forbidden). The anomalous mode with orbital number $l = 1$, which is

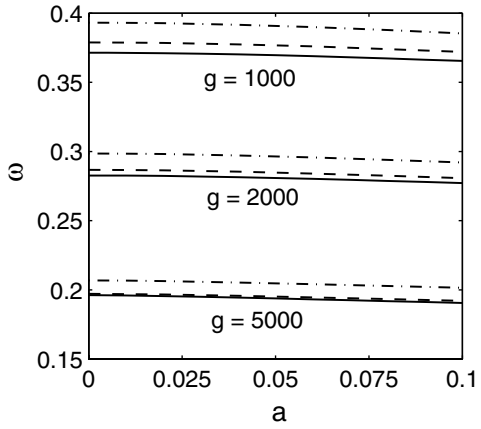

Figure 2. The frequency of the anomalous mode (for $\Omega = 0$) of the 1-vortex versus the interaction range for various values of the interaction strength for the perturbed harmonic trap (the parabolic potential perturbed by the quartic term), the dash and dash-dot lines. The solid line corresponds to the harmonic trap.

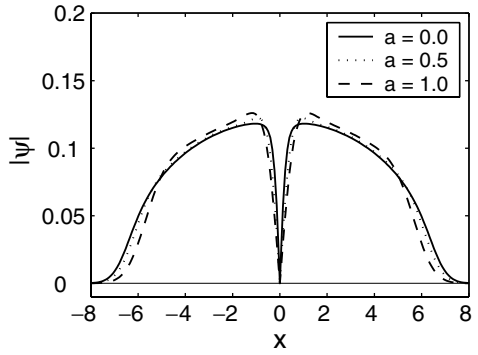

Figure 3. The shape of the 1-vortex solution for local, $a = 0$, and nonlocal, $a = 0.5, 1$, interactions. The interaction strength is $g = 3000$.

present for all axial n-vortices, has the closest to zero frequency for any range a ($\Omega = 0$). For the 2-vortex solution the instability intervals versus the interaction range are illustrated in figure 4. We found that with increasing interaction strength g the instability intervals move towards smaller values of the interaction range.

Nonlocality is also responsible for the appearance of additional anomalous modes with orbital numbers higher than the vorticity ($n < l < 2n$). For $\Omega = 0$ this happens for the axial n-vortices with $n \geqslant 2$, which have more than one orbital number l in the interval $0 < l < 2n$, where the operators H_l introduced in (23) may have negative eigenvalues. For the 2-vortex solution the additional anomalous mode has orbital number $l = 3$, see figure 5. For the 3-vortex solution, for instance, we have observed the creation of such an anomalous mode with $l = 5$. It should be noted that for some values of the interaction strength there are anomalous modes with higher orbital numbers in the local model as well. For instance, the axial 2-vortex solution has an anomalous mode with $l = 3$ for $g = 2000$. For the 3-vortex solution and $g = 10^4$ there is an anomalous mode with $l = 4$ (it resonantly collides with normal modes giving rise to instabilities, see below).

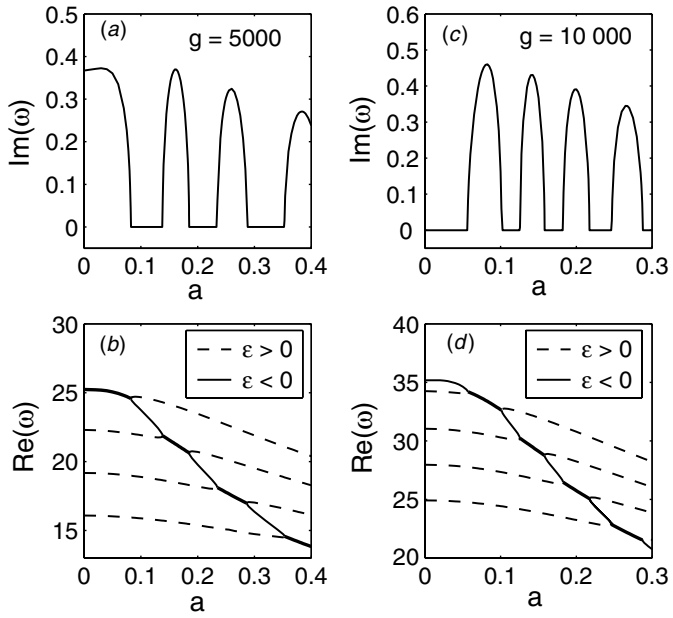

Figure 4. The real, (*b*) and (*d*), and imaginary, (*a*) and (*c*), parts of the eigenfrequencies corresponding to the orbital linear modes with $l = 2$ of the axial 2-vortex (here $\Omega = 0$). Only the anomalous mode and the resonant normal modes are shown (the insets give the signature). The 2-vortex solution loses its stability due to collision resonance of the anomalous mode (solid line) and the normal modes (dashed lines).

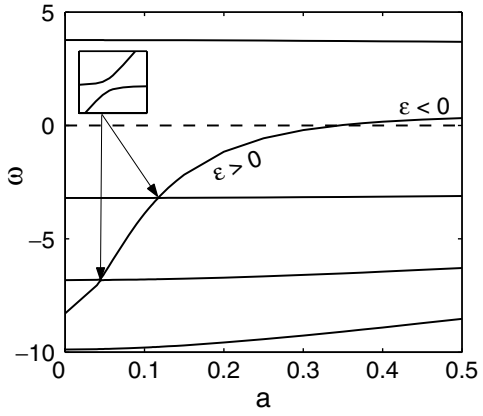

Figure 5. Zero crossing with the creation of an anomalous mode with the orbital number $l = 3$ of the axial 2-vortex. In the picture $g = 5000$ and $\Omega = 0$. The inset indicates the avoided crossing collisions of the normal modes.

The frequency of the created anomalous mode remains close to zero, therefore no resonances are possible with further increase of a. The threshold value of a at which the zero crossing occurs decreases with increasing interaction strength, for instance, for $g = 10^4$ the threshold is $a \approx 0.3$ compared to $a \approx 0.35$ for $g = 5 \times 10^3$ in figure 5.

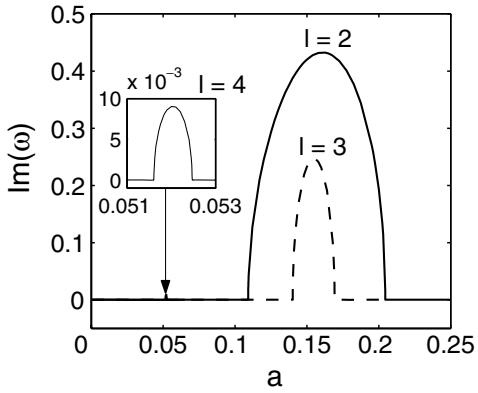

Figure 6. The imaginary part of the eigenfrequencies corresponding to the unstable orbital modes with the orbital numbers $l = 2$, 3 and $l = 4$ (in the inset) of the axial 3-vortex. Here the interaction strength is $g = 10^4$.

Finally, we have found that nonlocality opens new splitting channels for the axial n-vortex in the interval $n < l < 2n$. In contrast, as noted in [62], the instability channels of the axial n-vortices in the local GP equation satisfy $l \leqslant n$ with the symmetric splitting instability, $l = n$, being the strongest. The situation is different in the nonlocal model since there is an additional parameter—the range a. For instance, it is possible to find such values of the interaction strength and the range that the only dynamical instability of the axial n-vortex has orbital number higher than n. This happens already in the case of the 3-vortex, as seen from figure 6. However, the instabilities with the orbital numbers $l > n$ turn out to be weak. Similar, for the 4-vortex solution, we have found that for a close to 0.1 the only unstable orbital mode has the orbital number $l = 6$ with $\mathrm{Re}(\omega)$ of order 10^{-3}.

The new channels of instability with $n < l < 2n$ seem to suggest the existence of new non-axial vortex solutions, involving combinations of vortices and antivortices, which could minimize the energy for some rotation frequency. However, it turns out that in the nonlocal GP equation, similar to the local one, the stationary vortex solutions involving combinations of vortices and antivortices are never the energy minimizers—there always exists another stationary solution with the same total vorticity, but comprising vortices only, which minimizes the energy. For instance, the instability with $l = 4$ of the axial 3-vortex solution, shown in figure 6, could result in the formation of a non-axial 5-vortex solution with four vortices and one antivortex. Such a solution was indeed found by the minimization starting from the seed resembling the axial 3-vortex, see the right panel of figure 7. For rotation frequencies $\Omega > 0.38$ this solution has lower energy than the ground state; however, there is at least one other solution, the combination of three vortices, shown in the left panel of figure 7, which has lower energy than the vortex–antivortex solution for all rotation frequencies. It is interesting to note that both these solutions do exist in the local model ($a = 0$).

More complicated combinations of vortices and antivortices were found by the energy minimization. However, our numerical results indicate that for a stationary solution involving vortices and antivortices there always exists another stationary solution with the same total vorticity, but comprising vortices only, which has lower energy. This is true for the local and nonlocal GP equations. For instance, in figure 8 we give such solutions with total vorticity 8: the left panel shows the 8-vortex solution (the energy minimizer) and the right one shows the 16-vortex solution with 12 vortices and 4 antivortices.

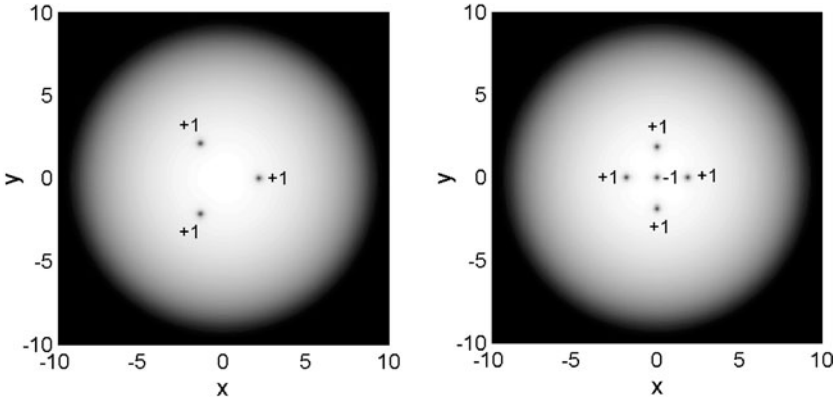

Figure 7. The stationary vortex solutions for $a = 0.052$, $g = 10^4$ and $\Omega = 0.38$. The left panel shows the 3-vortex solution and the right one shows the 5-vortex solution comprising four vortices and one antivortex (in the centre).

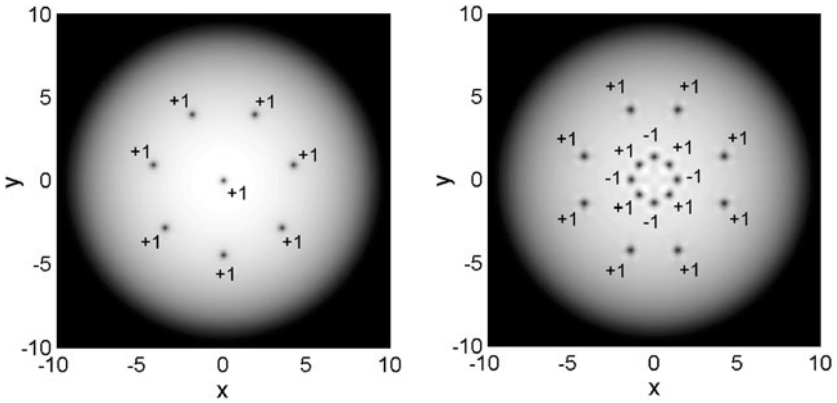

Figure 8. The stationary vortex solutions for $a = 0.052$, $g = 10^4$ and $\Omega = 0.5$. The left panel shows the 8-vortex solution and the right one shows the 16-vortex solution comprising 12 vortices and 4 antivortices.

Though the numerical simulations were performed on a modest personal computer, by employing the pseudo-spectral methods we nevertheless are able to resolve the phase of the solution and determine the positions and signs of all vortices by direct computation of the necessary contour integrals. Moreover, the estimate on the vortex size is in agreement with the numerics: for $g = 10^4$ used in figures 7 and 8 and the radial size of the ground state solution estimated as $R \sim 10$ (in dimensionless units), we get the healing length as $\xi \sim 0.03$ (compare with figures 7 and 8). However, the fine structure of the order parameter decay to zero at the centre of every single vortex cannot be resolved with due accuracy. This is manifested in the comparison of the left and right panels of figure 8, where in the left panel we give the solution on the grid 128×128, while in the right panel the solution computed on the grid 64×64 is refined by interpolation to the grid of the left panel. The strong coupling coefficients $g \geqslant 10^4$ require a lot more computer resources for resolution of the single vortex shape, when there are many vortices in the system. However, this is not the goal of the present publication.

5. Conclusion

In the present paper we have made an attempt to understand what changes in the properties of quantized vortices can be attributed to the range of interaction, when the latter is not negligible. The motivation was the similarity of the properties of quantized vortices in gaseous BECs, where the range of interactions is much smaller than the size of the vortex core and, hence, negligible, and in liquid helium, where the vortex core size is comparable to the interaction range.

In general, the local GP equation cannot be justified for a description of the quantized vortices in liquid helium. It is a common approach to use a nonlocal model for the phenomenological description of collective phenomena in such systems. However, there is only one local model and infinitely many nonlocal ones, if the derivation from the first principles is difficult or not possible to carry out. To choose between different nonlocal models one is left to rely on the analysis of each term in the model to understand the effect of it. In this paper we have analysed solely the effect of the finite range of interaction on the properties of quantized vortices. The interaction range affects the stability properties of the n-fold vortices creating new channels for vortex splitting. However it has only a slight effect on the threshold frequency above which the nonvortex state ceases to be the global energy minimum.

Here we note the difference in the effect of nonlocality in two-dimensional and one-dimensional GP equations. In 2D there is always a threshold value of the interaction range for the appearance of the instabilities caused solely by nonlocality, while, as suggested by numerical simulations in [71], in 1D such instabilities may set in beyond all orders of the range parameter.

Finally, in spite of the fact that the finite interaction range opens new splitting channels with the creation of antivortices, for any value of the interaction range and any rotation frequency for the vortex–antivortex solution there is a plain vortex solution of the same vorticity but with a lower energy. Thus, the annihilation of a vortex–antivortex pair lowers the energy, which will prevent the vortex–antivortex states from being observed. However, *a priori*, this is not evident, since there is mutual interaction between the individual vortices which depends on the model and is not known in detail at a small distance. In the local GP equation, for instance, the interaction potential is known only at large distance, and it has only the logarithmic fall-off according to the Kirchoff–Onsager formula. We can explain the insensitivity of the topological structure of the minimizers to the interaction range if we suppose that the leading term in the interaction potential is due to the phase overlap in the kinetic term (which, in fact, gives nothing but the Kirchoff–Onsager formula).

In connection with this, it would be interesting to find out what changes to the vortex interaction will bring the inclusion of a nonlinear and/or nonlocal correction to the kinetic energy in the density functional. Such corrections have been suggested in the literature on liquid helium (see, for instance, [46]). There will be significant changes in the structure of the energy minimizers as is suggested by a similar but completely integrable model which also admits vortex solutions—the Euclidean complex sine-Gordon equation. In the latter model the kinetic energy term is nonlinear, which results in energy degeneracy with respect to the number of vortices and antivortices as long as the total vorticity is fixed [72]. This is a direction for future studies.

Acknowledgments

This research was supported by the FAPESP grant. The authors are grateful to A M Kamchatnov for helpful discussions.

References

[1] Gross E P 1961 *Nuovo Cimento* **20** 454
[2] Pitaevskii L P 1961 *Zh. Eksp. Teor. Fiz.* **40** 646
Pitaevskii L P 1961 *Sov. Phys.—JETP* **13** 451 (Engl. Transl.)
[3] Dalfovo F, Giorgini S, Pitaevskii L P and Stringari S 1999 *Rev. Mod. Phys.* **71** 463
[4] Baym G and Pethick C J 1996 *Phys. Rev. Lett.* **76** 6
[5] Holland M and Cooper J 1996 *Phys. Rev.* A **53** R1954
[6] Anderson M H, Ensher J R, Matthews M R, Wieman C E and Cornell E A 1995 *Science* **269** 198
[7] Edwards M, Ruprecht P A, Burnett K, Dodd R J and Clark C W 1996 *Phys. Rev. Lett.* **77** 1671
[8] Jin D S, Ensher J R, Matthews M R, Wieman C E and Cornell E A 1996 *Phys. Rev. Lett.* **77** 420
[9] Andrews M R, Townsend C G, Miesner H-J, Durfee D S, Kurn D M and Ketterle W 1997 *Science* **275** 637
[10] Röhrl A, Naraschewski M, Schenzle A and Wallis H 1997 *Phys. Rev. Lett.* **78** 4143
[11] Matthews M R, Anderson B P, Haljan P C, Hall D S, Wieman C E and Cornell E A 1999 *Phys. Rev Lett.* **83** 2498
[12] Madison K W, Chevy F, Wohlleben W and Dalibard J 2000 *Phys. Rev. Lett.* **84** 806
Chevy F, Madison K W and Dalibard J 2000 *Phys. Rev. Lett.* **85** 2223
[13] Abo-Shaeer J R, Raman C, Vogels J M and Ketterle W 2001 *Science* **292** 476
[14] Raman C, Abo-Shaeer J R, Vogels J M, Xu K and Ketterle W 2001 *Phys. Rev. Lett.* **87** 210402
[15] Anderson B P, Haljan P C, Regal C A, Feder D L, Collins L A, Clark C W and Cornell E A 2001 *Phys. Rev. Lett.* **86** 2926
[16] Dutton Z, Buddle M, Slowe C and Hau L V 2001 *Science* **293** 663
[17] Hodby E, Hechenblaikner G, Hopkins S A, Maragò O M and Foot C J 2002 *Phys. Rev. Lett.* **88** 010405
[18] Haljan P C, Coddington I, Engels P and Cornell E A 2001 *Phys. Rev. Lett.* **87** 210403
[19] Leanhardt A E, Shin Y, Kielpinski D, Pritchard D E and Ketterle W 2003 *Phys. Rev. Lett.* **90** 140403
[20] Lundh E, Pethick C J and Smith H 1997 *Phys. Rev.* A **55** 2126
[21] Isoshima T and Machida K 1999 *Phys. Rev.* A **60** 3313
[22] Svidzinsky A A and Fetter A L 2000 *Phys. Rev. Lett.* **84** 5919
Feder D L, Svidzinsky A A, Fetter A L and Clark C W 2001 *Phys. Rev. Lett.* **86** 564
[23] Dalfovo F and Stringari S 2001 *Phys. Rev.* A **63** 011601
[24] Williams J E, Zaremba E, Jackson B, Nikuni T and Griffin A 2002 *Phys. Rev. Lett.* **88** 070401
[25] Penckwitt A A, Ballagh R J and Gardiner C W 2002 *Phys. Rev. Lett.* **89** 260402
[26] Mizushima T, Isoshima T and Machida K 2001 *Phys. Rev.* A **64** 043610
[27] Simula T P, Virtanen S M M and Salomaa M M 2002 *Phys. Rev.* A **66** 035601
[28] García-Ripoll J J and Pérez-García V M 1999 *Phys. Rev.* A **60** 4864
[29] García-Ripoll J J and Pérez-García V M 2001 *Phys. Rev.* A **63** 041603
[30] Crescimanno M, Koay C G, Peterson R and Walsworth R 2000 *Phys. Rev.* A **62** 063612
[31] Lundh E, Martikainen J P and Suominen K-A 2003 *Phys. Rev.* A **67** 063604
[32] Lieb E H, Seiringer R and Yngvason J 2000 *Phys. Rev.* A **61** 043602
[33] Lieb E H, Seiringer R and Yngvason J 2001 *Commun. Math. Phys.* **224** 17
[34] Lieb E H and Seiringer R 2002 *Phys. Rev. Lett.* **88** 170409
[35] Onsager L 1949 *Nuovo Cimento* **6** (Suppl. 2) 249 and 281
Feynman R P 1955 *Progress in Low Temperature Physics* vol 1, ed C J Gorter (Amsterdam: North-Holland) p 17
[36] Donnelly R J 1991 *Quantized Vortices in Helium II* (Cambridge: Cambridge University Press)
[37] Saffman P G 1992 *Vortex Dynamics* (Cambridge: Cambridge University Press)
[38] Balibar S 2003 Looking back at superfluid helium *Preprint* cond-mat/0303561
[39] Vinen W F 1961 *Proc. R. Soc.* A **240** 114
[40] Williams G A and Packard R E 1974 *Phys. Rev. Lett.* **33** 280
[41] Yarmchuck E J and Packard R E 1982 *J. Low Temp. Phys.* **46** 479
[42] Dalfovo F and Stringari S 2001 *J. Chem. Phys.* **115** 10078
[43] Stringari S and Treiner J 1987 *Phys. Rev.* B **36** 8369
Stringari S and Treiner J 1987 *J. Chem. Phys.* **87** 5021
[44] Dupont-Roc J, Himbert M, Pavloff N and Treiner J 1990 *J. Low Temp. Phys.* **81** 31
[45] Dalfovo F 1992 *Phys. Rev.* B **46** 5482
[46] Dalfovo F, Lastri A, Pricaupenko L, Stringari S and Treiner J 1995 *Phys. Rev.* B **52** 1193
[47] Berloff N G and Roberts P H 1999 *J. Phys. A: Math. Gen.* **32** 5611
[48] Berloff N G 1999 *J. Low Temp. Phys.* **116** 359

[49] Jones C A and Roberts P H 1982 *J. Phys. A: Math. Gen.* **15** 2599
[50] Frisch T, Pomeau Y and Rica S 1992 *Phys. Rev. Lett.* **69** 1644
[51] Koplik J and Levine H 1993 *Phys. Rev. Lett.* **71** 1375
Koplik J and Levine H 1996 *Phys. Rev. Lett.* **76** 4745
[52] Nore C, Brachet M E and Fauve S 1993 *Physica* D **65** 154
[53] Berloff N G and Roberts P H 2000 *Phys. Lett.* A **274** 69
[54] Pérez-García V M, Konotop V V and García-Ripoll J J 2000 *Phys. Rev.* E **62** 4300
[55] Parola A, Salasnich L and Reatto L 1998 *Phys. Rev.* A **57** R3180
[56] Salasnich L 1999 *Phys. Rev.* A **61** 015601
[57] Lebedev N N 1972 *Special Functions and Their Applications* (New York: Dover)
[58] Svidzinsky A A and Fetter A L 2000 *Phys. Rev. Lett.* **84** 5919
Svidzinsky A A and Fetter A L 1998 *Phys. Rev.* A **58** 3168
[59] Rokhsar D 1997 *Phys. Rev. Lett.* **79** 2164
[60] Dodd R J, Burnett K, Edwards M and Clark C W 1997 *Phys. Rev.* A **56** 587
[61] Skryabin D V 2000 *Phys. Rev.* A **63** 013602
[62] Pu H, Law C K, Eberly J H and Bigelow N P 1999 *Phys. Rev.* A **59** 1533
[63] Saito H and Ueda M 2002 *Phys. Rev. Lett.* **89** 190402
[64] Aranson I S and Steinberg V 1996 *Phys. Rev.* B **53** 75
[65] Gabbay M, Ott E and Guzdar P N 1997 *Phys. Rev. Lett.* **78** 2012
[66] Aranson I S and Bishop A R 1997 *Phys. Rev. Lett.* **79** 4174
[67] Kivshar Yu S and Luther-Davis B 1998 *Phys. Rep.* **298** 81
[68] Mackay R S 1987 *Hamiltonian Dynamical Systems* ed R S Mackay and J D Meiss (Bristol: Hilger) p 137
[69] For introduction to the pseudospectral methods consult Fornberg B 1996 *A Practical Guide to Pseudospectral Methods* (Cambridge: Cambridge University Press)
Boyd J P 2000 *Chebyshev and Fourier Spectral Methods* 2nd edn (New York: Dover)
Trefethen L N 2000 *Spectral Methods in Matlab* (Philadelphia, PA: SIAM)
[70] Shchesnovich V S The generalized Rayleigh quotient for nonlinear systems in preparation
[71] Deconinck B and Kutz J N 2003 *Phys. Lett.* A **319** 97
[72] Barashenkov I V, Shchesnovich V S and Adams R 2002 *Nonlinearity* **15** 2121